

Research on UAVs Reconnaissance Task Allocation Method Based on Communication Preservation

Xueqing Li[✉], Graduate Student Member, IEEE, Xinpeng Lu[✉], Wenhao Chen[✉], Die Ge, and Junwu Zhu[✉]

Abstract—The research on multi-UAV reconnaissance task allocation is of great significance for both military and civilian fields. Existing methods simplify targets as points and ignore the heterogeneity of shape and values. Motivated by this oversight, a reconnaissance strategy is proposed for each type of heterogeneous target. Based on the proposed strategy, the reconnaissance information revenue function is formalized considering the correlation between target and time. Additionally, the utility of UAVs depends on the revenue of information and flight costs. The Heterogeneous Target Reconnaissance Allocation (HTRA) scheme is designed to optimize the utility. Specifically, the resource matching matrix model was firstly used to realize initial allocation. Subsequently, the sequence of tasks is optimized by using the Improved Particle Swarm Optimization (IPSO) algorithm. Finally, the reconnaissance time is optimized by Gradient Projection (GP) algorithm to improve the utility of UAVs. Moreover, the HTRA scheme is expanded to HTRA⁺, and a communication preservation-based auction method is proposed to address limited communication in UAVs cooperation. The experiment results show that the proposed scheme outperforms existing methods in terms of reconnaissance utility and the rate of task completion.

Index Terms—Task allocation, heterogeneous targets, reconnaissance utility, communication preservation.

I. INTRODUCTION

THE UNMANNED Aerial Vehicle (UAV), a new type of equipment, can replace human pilots for boring and dangerous tasks [1], [2]. With their maneuverability and flexibility, UAVs are widely used in reconnaissance [3], inspection [4], search [5], rescue [6], [7], and monitoring [8]. However, a single UAV has limited capabilities in handling intricate tasks [9]. In recent years, experts from various fields have been researching effective collaboration among UAVs. Task allocation plays a crucial role in determining the

Manuscript received 23 November 2023; revised 8 January 2024; accepted 18 February 2024. Date of publication 21 February 2024; date of current version 26 April 2024. This work was supported in part by the National Natural Science Foundation of China under Grant 61872313; in part by the Postgraduate Research and Practice Innovation Program of Jiangsu Province under Grant KYCX18_2366; in part by the Innovation and Entrepreneurship Training Program for College Students in Jiangsu Province under Grant 202311117059Z; in part by the Yangzhou Science and Technology under Grant YZ2018209 and Grant YZ2019133; in part by the Special Innovation Fund for Medical Innovation and Transformation – Clinical Translational Research Project of Yangzhou University under Grant AHYZUZHXM202103; and in part by the Science and Technology on Near-Surface Detection Laboratory under Grant 6142414220509. (*Corresponding author: Junwu Zhu.*)

The authors are with the Department of Information Engineering, Yangzhou University, Yangzhou 225127, China (e-mail: dx120200080@stu.yzu.edu.cn; 211301216@stu.yzu.edu.cn; 212308213@stu.yzu.edu.cn; mx120210561@stu.yzu.edu.cn; jwzhu@yzu.edu.cn).

Digital Object Identifier 10.1109/TCE.2024.3368062

success of UAV tasks [10]. Reasonable task allocation enables orderly execution of tasks, reduces system costs, and improves efficiency [11].

The task allocation problem of UAVs is NP-hard [12]. Common models for solving this problem include Multiple Traveling Salesman Problem [13] and Vehicle Routing Problem [14], but they are not effective for complex optimization problems. Therefore, alternative optimization models such as Dynamic Programming [15], Mixed-Integer Linear Programming [16], and Cooperative Multiple Task Allocation Problem [17] have been proposed to handle complex scenarios. In terms of task allocation methods, commonly used algorithms include swarm intelligence optimization algorithms [18] and market mechanism-based algorithms [19]. Swarm intelligence algorithms can provide approximate optimal solutions at an acceptable computational cost. Currently, popular swarm intelligence algorithms include Ant Colony Optimization [20] and Particle Swarm Optimization (PSO) [21]. Compared with other optimization algorithms, PSO has good global search ability, higher probability of finding the global optimal solution, and faster convergence speed. In task allocation, game theory and auction are also common solutions. Qi et al. [22] proposed to optimize collaborative task resource allocation by designing a game model. Market mechanism-based algorithms mainly consist of the contract network algorithm [23] proposed by Smith in 1980 and the auction algorithm [24] proposed by Bertsekas in 1981. In recent years, auction methods provide new ideas for multi-UAV data collection [25], [26].

The reconnaissance task is crucial for both military and civilian UAVs. However, the current allocation of these tasks often overlooks the relationship between reconnaissance benefits and time. Existing models mainly focus on minimizing costs or maximizing total task value [27], without considering the connection between reconnaissance revenue and time. Generally, as the duration of reconnaissance increases, more information is gathered by UAVs. Additionally, most existing task allocation models prioritize UAV characteristics while oversimplifying geometric properties of reconnaissance targets [28]. As a result, these reconnaissance models may not be effectively applicable in real-world scenarios.

The proposed UAVs task allocation scheme, HTRA, addresses challenges faced by UAVs in executing coordinated reconnaissance tasks involving heterogeneous targets, lack of correlation between reconnaissance revenue and time, and communication limitations. HTRA considers the heterogeneity of UAVs reconnaissance target geometry and value to

maximize reconnaissance information. Moreover, it combines reconnaissance revenue with time to improve task efficiency for heterogeneous targets. Furthermore, the HTA framework is extended to cater to communication-limited scenarios, enhance task completion rate, and ensure integrity of reconnaissance information acquisition. The primary contributions of this study are as follows:

- 1) The proposed strategy for UAVs based on heterogeneous targets, alongside the establishment of a UAVs reconnaissance revenue model that is contingent upon the duration of reconnaissance time.
- 2) The study proposes a HTA model to address the heterogeneous reconnaissance target assignment problem. The algorithm simplifies the complex problem by matching matrix, and uses an Improved PSO (IPSO) algorithm and a reconnaissance time allocation algorithm based on Gradient Projection (GP) to determine the task execution order and reconnaissance time allocation.
- 3) The HTA⁺ model addresses the issue of limited communication during subsequent UAV tasks. The effectiveness of the algorithm is validated through experimental analysis in diverse scenarios.

The paper is organized as follows: Section II describes the research related to UAVs task allocation. Section III presents a formal model and algorithm for allocating reconnaissance tasks to UAVs. In Section IV, comparative experiments are carried out through numerical simulations. Section V discusses the effectiveness of the proposed HTA⁺ model in communication preservation. Finally, Section VI summarizes the work.

II. RELATED WORK

Task allocation involves considering task requirements and UAVs characteristics to establish a rational mapping between UAVs and tasks. To address the cooperative task planning problem for UAVs, Du et al. [29] proposed a hierarchical optimization scheme based on the k-means clustering method for task allocation and path optimization of UAVs. Jiang et al. [30] introduced an optimal ordering strategy based on dominance rough sets, enabling hierarchical task allocation for different sizes of UAVs and tasks. Zhang et al. [31] presented the fully adaptive cross entropy algorithm, which determines feasible solutions based on resource constraints and priority constraints to handle the problem of UAV task allocation. To enhance the completion rate of task execution, Li et al. [32] devised an efficient Establishment Quantum Particle Swarm Optimization coalition scheduling algorithm by utilizing similarity judgments to reduce time overhead in coalition formation. Amorim et al. [33] proposed a heuristic algorithm that combines group intelligence strategy with the Generalized Assignment Problem (GAP) approach to improve the completion rate of tasks executed by UAVs. In their study on reconnaissance tasks performed by UAVs, Wei and Zhao [34] classified reconnaissance targets into high-value targets, low-value targets, and decoy targets; they employed the Mean-Variance Optimization (MVO) algorithm to solve the problem of reconnaissance task allocation under

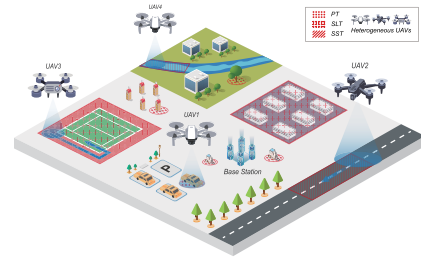


Fig. 1. UAVs cooperative target reconnaissance model.

varying target values. Zhu et al. [35], put forward an inverse genetic algorithm based on two-chromosome coding and multi-mutation operator to enhance global search capability in their algorithm design. Gao et al. [36], meanwhile, proposed a meta-heuristic algorithm based on Grouped Ant Colony Optimization (GACO) algorithm to tackle heterogeneous reconnaissance target allocation.

The aforementioned research demonstrates that the field of multi-UAV task allocation cooperation has been extensively investigated both domestically and internationally, yielding fruitful outcomes. However, certain challenges still remain to be addressed. In most of the above studies, the targets are predominantly considered homogeneous [29], [30], [31], without accounting for the heterogeneity of targets and UAVs in real scenarios [31], [34], thereby neglecting the heterogeneity in target value [29], [30], [31], [34], [35]. While existing studies on target heterogeneity primarily focus on value differences [34], [35], the enemy command has a higher reconnaissance value than ordinary air-to-ground ones. In studies that consider the heterogeneity of geometry of targets [35], the reconnaissance values are often considered to be the same, which is not consistent with the real reconnaissance scenarios. The literature [32], [33] fails to consider the issue of communication limitations during the execution of subsequent tasks when assessing the completion rate of UAV task execution. Currently, in the research for reconnaissance tasks [36], the reconnaissance task is regarded as an ordinary task, which does not take into account the characteristics of target and ignores the impact of reconnaissance time on revenue.

Therefore, it is imperative to develop a task allocation model for UAV reconnaissance tasks that takes into account the following factors: heterogeneity of UAVs, geometry of reconnaissance targets, variability in target value, temporal correlation with revenue, and communication preservation.

III. DESCRIPTION OF THE PROBLEM

The study presents a UAVs reconnaissance system, consisting of a Base Station (*BS*) and N UAVs as depicted in Fig. 1. The system is designed to cooperatively execute the reconnaissance tasks of a region with complex terrain and M targets. UAVs are employed to carry out reconnaissance tasks by using sensors on targets within the region. To optimize the traversal planning of UAVs for all targets while considering their performance characteristics and endurance time, the reconnaissance and hovering duration and sequence for each target are determined under cost constraints aiming

TABLE I
NOTATION TABLE

d	sensor detection diameter
N, M	number of UAVs, targets
L_T, W_T	the length and width of the target
Z_T	total search path length
S_T	area of the target
t_i	reconnaissance time for target $_i$
I_i	information acquired from target $_i$
I_{ki}	information known prior
I_{ui}	uncertain information part
$\delta(t_i)$	information amount function
A_i	UAVs reconnaissance resource utilization
G	total utility of UAVs
C_j	the cost of UAV $_j$
P_j	sequence of targets for UAV $_j$
Tf_j	the flight time of UAV $_j$

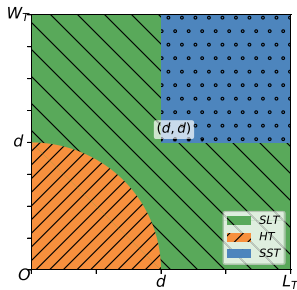


Fig. 2. Diagram of heterogeneous reconnaissance target differentiation.

to maximize the total utility of UAVs. The common notations in the proposed model are shown in Table I.

A. Heterogeneous Target Reconnaissance Strategy

Reconnaissance targets are often treated as mere points in common models, overlooking the geometric characteristic of targets that cannot be adequately represented as points. In this paper, the UAV is equipped with a reconnaissance sensor to detect ground targets. It is assumed that the field of view of the sensor is a circle with radius r , diameter $d = 2r$. L_T, W_T and S_T are used to describe the reconnaissance target length, width and area, respectively. To simplify the model, it is assumed that the sensor's field of view remains unaffected by the UAV's attitude and that each UAV maintains a constant speed during transitions between targets.

According to the geometric characteristics of the reconnaissance target and the sensor's field of view, it is possible to determine the appropriate heterogeneous reconnaissance strategy, as depicted in Fig. 2. Furthermore, the reconnaissance strategies for heterogeneous targets can be categorized into fixed-point hovering, straight-line flight, and S-shaped flight, as illustrated in Figs. 3, 4 and 5.

The Hover Target(HT) is shown in Fig. 3, and the fixed-point hovering strategy is used when the size of the target falls below the sensor's field of view. It is employed for reconnaissance of targets with dimensions smaller than the sensor's field of view, such as buildings and ground vehicles. Take the case $L_T > W_T$ as an example. When the area length $L_T < d$ and the width $W_T < \sqrt{d^2 - L_T^2}$, the reconnaissance sensor can directly cover the entire area.



Fig. 3. Fixed-point hovering strategy.

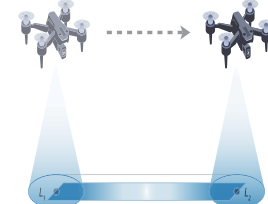


Fig. 4. Straight-line flight strategy.

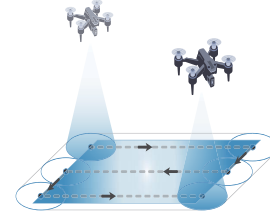


Fig. 5. S-shaped flight strategy.

Typical straight-line targets (SLTs), such as railways, rivers, and airstrips, are illustrated in Fig. 4. Next, the analysis of $L_T > W_T$ reveals two distinct cases in the straight flight strategy.

- Case 1: target length $L_T > d$ and width $0 < W_T < d$;
- Case 2: target length $\frac{\sqrt{2}}{2}d < L_T < d$ and width $\sqrt{d^2 - L_T^2} < W_T < L_T$.

In the following, the focus of this study lies in designing an optimal search path that ensures complete coverage of the target while minimizing flight costs.

Theorem 1: The UAV can achieve the shortest path while ensuring complete coverage of the line target by flying over the midline along its longer edge.

Proof: Consider the line path separately in two cases:

Case 1: When the length of the target $L_T > d$, full coverage of the target cannot be achieved if the UAV flies straight along the shorter edge. However, if the UAV flies straight along the longer edge, the Z_T is:

$$Z_T = L_T - 2\sqrt{r^2 - W_T^2/4} \quad (1)$$

Case 2: If the UAV flies straight along the shorter edge, the Z_T is:

$$Z_{T_1} = W_T - 2\sqrt{r^2 - L_T^2/4} \quad (2)$$

On the other hand, if the UAV flies straight along the longer edge, the Z_T is:

$$Z_T = L_T - 2\sqrt{r^2 - W_T^2/4} \quad (3)$$

When $L_T > W_T$, it is observed that $Z_{T_1} > Z_{T_2}$, indicating that the UAV has a shorter search path when flying along a longer edge. It can be inferred that the UAV employs the flight strategy of flying along the longer edge of the SLT. Therefore, the expression for the shortest search path Z_T is as follows:

$$Z_T = \begin{cases} W_T - \sqrt{d^2 - L_T^2}, & L_T \leq W_T \\ L_T - \sqrt{d^2 - W_T^2}, & L_T > W_T \end{cases} \quad (4)$$

As depicted in Fig. 5, when the dimensions of the Target exceed a threshold value d , the UAV employs an S-shaped reconnaissance strategy to minimize flight path cost, referred to as S-Shaped Target (SST).

The UAV determines the entrances and exits based on the four vertices. The reconnaissance path length of the UAV can be mathematically formulated as follows:

$$Z_T = \begin{cases} [[L_a/d]([W_a/d] - 1)] \times d, & L_T \leq W_T \\ [[W_T/d]([L_T/d] - 1)] \times d, & L_T > W_T. \end{cases} \quad (5)$$

B. Information Revenue Model

The purpose of UAV reconnaissance on the targets is to gather valuable information and reduce the uncertainty of these targets. The reconnaissance time vector is denoted as $\mathbf{t} = (t_1, t_2, \dots, t_M)$. $\delta(t_1, t_2, \dots, t_M)$ relates the reconnaissance times to the amount of information acquired on different targets. Therefore, the final information acquired for all targets can be represented as a vector $\mathbf{I} = (I_1, I_2, \dots, I_M)$, where

$$I_i = I_{ki} + A_i \cdot I_{ui} \frac{e^{t_i} - 1}{e^{t_i} + 1} \quad (6)$$

I_i represents the total information revenue obtained by reconnaissance of the i -th task. Here, $I_{ki} + I_{ui} = 1$. I_{ki} represents the known information of the UAV to the task before the reconnaissance starts (for example, through satellite or historical data collection), and I_{ui} represents the information uncertainty part of the UAV to the task. During the UAV's task, the actual area should completely cover the target area S_T . If the actual area is much larger than S_T , there will be a waste of reconnaissance resources. The UAV reconnaissance resource utilization A_i is defined as the ratio of the target area S_T to the actual reconnaissance area. Formally, it can be expressed as follows:

$$A_i = \begin{cases} \frac{S_T}{\pi r^2}, & \text{Case 1} \\ \frac{S_T}{\pi r^2 + 2rZ_T}, & \text{Case 2} \\ \frac{S_T}{\pi r^2 + S_T + 2r \max\{L_T, W_T\}}, & \text{Case 3} \end{cases} \quad (7)$$

For the three reconnaissance strategies, the utilization rate of reconnaissance resources can be categorized into the following three scenarios:

Case 1: When using the HT strategy, the actual reconnaissance area of the UAV is πr^2 .

Case 2: When using the SLT strategy, the actual reconnaissance area of the UAV is $\pi r^2 + 2rZ_T$.

Case 3: When using the SST strategy, the actual reconnaissance area of the UAV is $\pi r^2 + S_T + 2r \max\{L_T, W_T\}$.

The amount of information $\delta(\mathbf{t})$ can be expressed as follows:

$$\delta(\mathbf{t}) = \sum_{i=1}^M \left(I_{ki} + A_i \cdot I_{ui} \frac{e^{t_i} - 1}{e^{t_i} + 1} \right) \quad (8)$$

It's evident that the longer the reconnaissance duration, the more reconnaissance information is acquired. The total UAVs reconnaissance revenue in the model is the sum of the amount of information from all targets.

C. Problem Model

The reconnaissance revenue of a UAV on a target primarily relies on the acquisition of reconnaissance information during task execution. This information acquisition is closely associated with the duration spent by the UAV on the target. Based on the aforementioned analysis, it is proposed quantifying the reconnaissance revenue of a UAV by considering target information, which includes initial data obtained prior to entering the target area. As time progresses, there is an incremental improvement in certainty regarding acquired information. When certainty reaches 1, it signifies that complete establishment of target information has been achieved.

When UAV is allocated to execute a reconnaissance task, the total utility obtained by the UAVs system is influenced by the revenue gained and the flight costs. The parameters α and β represent the weighting factors for the reconnaissance information revenue and the flight costs, respectively. The cost of the UAVs is directly proportional to the duration of its usage, assuming constant unit fuel consumption. To streamline the model, the UAVs' cost can be represented as the aggregate of its operational hours. The problem of UAV reconnaissance is formulated as follows:

$$G_{\max} = \max \left(\alpha \sum_{i=1}^M I_i - \beta \sum_{j=1}^N C_j \right) \quad (9)$$

where, G represents the total utility of UAVs engaged in reconnaissance tasks, $\alpha \sum_{i=1}^M I_i$ denotes the cumulative information revenue obtained from M targets, and $\beta \sum_{j=1}^N C_j$ signifies the overall flight costs incurred by UAVs.

$$C_j = \sum_{k=1}^{|P_j|} t_{p_{j,k}} + \frac{1}{v_0} \left[d(p_{j,|P_j|}, p_{j,0}) + \sum_{k=0}^{|P_j|-1} d(p_{j,k}, p_{j,k+1}) \right] \quad (10)$$

Equation (10) represents the cost for UAV_j , which includes both targets reconnaissance time and flight time between targets. Here, $\sum_{k=1}^{|P_j|} t_{p_{j,k}}$ denotes the total time spent on targets reconnaissance, $P_j = \{p_{j,1}, \dots, p_{j,k}, \dots, p_{j,|P_j|}\}$ represents the sequence of reconnaissance targets for UAV_j (where $p_{i,k}$ refers to the k -th reconnaissance target), $d(p_{j,|P_j|}, p_{j,0})$ indicates the distance traveled by UAV_j back to base station after completing its last task, and $d(p_{j,k}, p_{j,k+1})$ represents the distance between exit point of k -th target for UAV_j and entrance point

of UAV_j and the entrance of the $(k+1)$ -th target. Here, $k=0$ corresponds to the distance traveled by the UAV from the base station to the first reconnaissance target. The constant flight speed of the UAV between targets is denoted by v_0 .

The constraints of the model are as follows:

$$|P_j| \neq 0, \forall j \quad (11)$$

$$P_i \cap P_j = \emptyset, \forall i \neq j \quad (12)$$

$$\sum_{j=1}^N |P_j| = M \quad (13)$$

$$p_{j,k} \in \{1, 2, \dots, M\}, \forall j, k \quad (14)$$

$$\frac{C_j}{\beta} \leq T_f \quad (15)$$

$$t_{p_{j,k}} \geq 0 \quad (16)$$

$$\text{Type}_{p_{j,k}}^T = \text{Type}_j^U, \forall p_{j,k} \in P_j \quad (17)$$

Constraint (11) ensures that UAV_j must include at least one target in its reconnaissance sequence P_j . Constraint (12) ensures that the sets of reconnaissance targets for all UAVs must have no common elements. Constraint (13) and (14) impose constraints on the total number of allocated targets and the range of target indices. Constraint (15) guarantees that the reconnaissance time of UAV_j on a target does not exceed its flight time T_f , which is limited by the UAV's energy resources. Constraint (16) ensures effective reconnaissance on each target, requiring non-negative time for target reconnaissance. Constraint (17) represents an objective type bound, which depends on maintaining consistency between UAV types.

D. The HTRA Model

In this section, the HTRA model is proposed to address the task allocation problem in complex scenarios. The model consists of three modules: resource-demand matrix matching model, initial allocation phase and reallocation phase.

1) Resource-Demand Matrix Matching Model: A resource-demand matrix matching model is designed as the basis for heterogeneous UAV reconnaissance task allocation. The proposed model is able to efficiently match tasks with suitable UAVs based on their specific capabilities and target geometry. The target demand matrix M_{Target_i} and UAV resource matrix M_{UAV_j} are expressed as follows: $M_{\text{Target}_i} = [T_i, \text{Type}_i^T, L_i^T, W_i^T, loc_i]$, $M_{\text{UAV}_j} = [U_j, \text{Type}_j^U, r_j, T_f]$. Here, T_i denotes the number of reconnaissance target i , and U_j represents the number of the UAV_j . In the demand matrix, Type_i^T represents the type of UAV required for the reconnaissance target i . loc_i represents the geographic location of the target, and Type_j^U represents the type of UAV_j . The proposed resource-demand matrix matching model is shown in **Algorithm 1**.

Utilizing the concept of bucket classification, **Algorithm 1** classifies UAVs and targets. Each entity is assigned to a specific bucket based on its type or demand, ensuring that each bucket contains entities of the same type. This approach facilitates the matching between UAVs and target demand types, resulting in the identification of UAV buckets and target buckets, along with a corresponding matching result matrix.

Algorithm 1 The Resource-Demand Matrix Matching Algorithm

Input: UAVs resource matrix M_{UAV} and reconnaissance targets demand matrix M_{Target}

Output: The buckets of UAV B_{UAV} , the buckets of target B_{Target} and matching result matrix $Z_{\text{match}} = \{z_{i,j}\}_{M \times N}$

```

1: Initialize:  $B_{\text{UAV}}^\lambda, B_{\text{Target}}^\lambda \leftarrow \emptyset, \forall \lambda \in \{\text{Type}_i^T \cup \text{Type}_j^U\}, z_{i,j} \leftarrow 0$ 
2: for each  $\text{UAV}_j$  in  $M_{\text{UAV}}$  do
3:    $\lambda_1 \leftarrow \text{Type}_j^U$ 
4:    $B_{\text{UAV}}^{\lambda_1} \leftarrow B_{\text{UAV}}^{\lambda_1} \cup M_{\text{UAV}_j}$ 
5:   for each Target $_i$  in  $M_{\text{Target}}$  do
6:      $\lambda_2 \leftarrow \text{Type}_i^T$ 
7:      $B_{\text{Target}}^{\lambda_2} \leftarrow B_{\text{Target}}^{\lambda_2} \cup M_{\text{Target}_i}$ 
8:     if  $\text{Type}_i^T = \text{Type}_j^U$  then
9:        $z_{i,j} \leftarrow 1$ 
10:    end if
11:   end for
12: end for

```

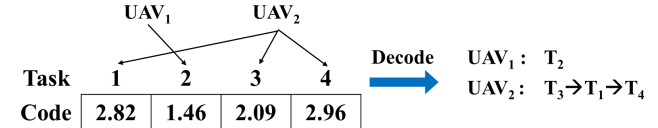


Fig. 6. Example of IPSO encoding and decoding.

2) Initial Allocation Phase: In the initial allocation phase, the model employed the IPSO algorithm to transform the feasible task allocation scheme into particles within the PSO framework. This algorithm employs real number coding to determine the solution of the UAV task sequence and facilitates efficient task allocation among UAVs.

Renumbering the set of matched UAVs and tasks sequentially, where $n_{\text{Type}_\lambda}^U$ represents the number of UAVs of type Type_λ , and $n_{\text{Type}_\lambda}^T$ denotes the count of reconnaissance targets requiring UAVs of type Type_λ . Each particle adopts a double-layer matrix structure, the first row of the matrix indicates the task number to be assigned. The second row of the matrix is represented by real number encoding in the interval $[1, n_{\text{Type}_\lambda}^U + 1]$, where the integer part of the real number is indicated the number of UAVs executing the task. At the same time, the size of the fractional part indicates the order of the UAVs executing the task, and the smaller the number indicates that the task is executed first. The initial particle swarm is formed by utilizing randomly generated double-layer matrix particles as feasible solutions. This matrix encoding ensures the execution of each target only once, determines the assignment of each target and the order of tasks, and maintains the feasibility of individual particles during position and velocity updates.

As depicted in Fig. 6, the integer part of task 2 is 1, and the integer parts of tasks 1, 3 and 4 are 2. This implies that UAV_1 executes task 2, while UAV_2 executes tasks 1, 3 and 4. Subsequently, the encoded particles should be decoded in order to determine the sequential task order for each UAV.

For instance, task 3 has a fractional part of 0.09, making it the first task to be executed. Next in line is task 1, with a fractional part of 0.82, and so on. This process enables each UAV to acquire the task sequence performed, facilitating the identification of task entry and exit points on the shortest path based on their respective sequences.

IPSO achieves the optimal solution by utilizing the inertia of each particle and learning from individual and population best solutions. Assume that the search space in which the target is located is D -dimensional, and the population size is $N_{\text{particles}}$. The position and velocity of particle i at the k -th iteration are given by:

$$X_{id}^k = [X_{i,1}^k, X_{i,2}^k, \dots, X_{i,D}^k], V_{id}^k = [V_{i,1}^k, V_{i,2}^k, \dots, V_{i,D}^k] \quad (18)$$

The update equation for the particle velocity can be expressed as:

$$V_{id}^{k+1} = \omega V_{id}^k + c_1 r_1 (P_{id}^k - X_{id}^k) + c_2 r_2 (G_{id}^k - X_{id}^k) \quad (19)$$

$$X_{id}^{k+1} = X_{id}^k + V_{id}^{k+1} \quad (20)$$

where ω indicates the inertia weight, k is the number of iterations, c_1 and c_2 are the learning factors, c_1 denotes the learning ability of the particle itself, c_2 denotes the learning ability of the group, and r_1 and r_2 are random numbers in the interval $[0, 1]$. Each particle evaluates its advantages and disadvantages through the fitness function and iterates. The fitness function corresponds to the objective function in Equation (17) and is expressed as:

$$f = \alpha \sum_{i=1}^M I_i - \beta \sum_{j=1}^N C_j \quad (21)$$

PSO converges faster, but it is easy to fall into local optimization in the late stage, this paper introduces adaptive inertia weights and learning factor mechanism on its basis. The inertia weights ω_k are set as:

$$\omega_k = -4(\omega_{\max} - \omega_{\min}) \left[\left(\frac{k}{k_{\max}} \right)^2 - \frac{k}{k_{\max}} \right] + \omega_{\min} \quad (22)$$

When $1 < k < k_{\max}/2$, the number of learning factors is set as $c_1 = c_{\max}$ and $c_2 = c_{\min}$. When $k_{\max}/2 < k < k_{\max}$, the number of learning factors is set as $c_1 = c_{\min}$ and $c_2 = c_{\max}$. Here k_{\max} is the maximum number of iterations and $\omega_{\min}, \omega_{\max}, c_{\min}, c_{\max}$ are the four unequal constants.

The improved algorithm enhances global search capability in the early stage by using a larger c_1 to promote learning from individual best solutions. In the later stage, it strengthens local search capability by using a larger c_2 to facilitate learning from the population best solution. The dynamic inertia weight prevents the algorithm from getting stuck in local optima during the later stages.

The IPSO algorithm is employed to plan tasks for the subproblems obtained through successful matrix matching in HTA. The algorithm iteratively optimizes the particle positions and ultimately discovers the globally optimal solution.

Algorithm 2 HTA Algorithm

Input: UAV resource matrix M_{UAV} and reconnaissance target demand matrix M_{Target}

Output: UAV reconnaissance task execution sequence and reconnaissance task allocation time

- 1: Resource-demand matching is realized, as detailed in **Algorithm 1**
- 2: Initialization: Number of particles $N_{\text{particles}}$, iterations k_{\max} , the position of particle X and the velocity of particle V
- 3: **for** $k = 1$ to k_{\max} **do**
- 4: Calculate adaptive inertia weight ω_k and learning factors c_1, c_2
- 5: **for** each particle $i = 1, \dots, N_{\text{particles}}$ **do**
- 6: Calculate the fitness value f_i
- 7: **if** $f_i < f_{P_i}$ **then**
- 8: $P_i \leftarrow X_i$
- 9: **end if**
- 10: **if** $f_i < f_{G_i}$ **then**
- 11: $G_i \leftarrow X_i$
- 12: **end if**
- 13: Generate the factor randomly $r_1, r_2 \in [0, 1]$
- 14: $V_i \leftarrow \omega_k V_i + c_1 r_1 (P_i - X_i) + c_2 r_2 (G_i - X_i)$
- 15: $X_i \leftarrow X_i + V_i$
- 16: **end for**
- 17: The optimal particle G_i is decoded
- 18: The reconnaissance time is allocated to the decoded task sequence according to **Algorithm 3**
- 19: **end for**

3) *Reallocation Phase*: The present section proposes a time allocation method for reconnaissance targets based on the GP algorithm. In addition to determining the execution sequence of UAV reconnaissance missions, it also determines the required time for each target to be surveyed by UAVs.

According to the problem model, it is assumed that the UAV $_j$ executes sequentially the task sequence $P_j = \{p_{j,1}, \dots, p_{j,k}, \dots, p_{j,|P_j|}\}$ and the total utility of the reconnaissance task is

$$G_j = \sum_{k=1}^{|P_j|} [\alpha \delta(t_{p_{j,k}}) - \beta t_{p_{j,k}}] - \frac{\beta}{v_0} \left[d(p_{j,k}, p_{j,0}) + \sum_{k=0}^{|P_j|-1} d(p_{j,k}, p_{j,k+1}) \right] \quad (23)$$

In the process of reconnaissance task execution, the duration time of reconnaissance not only affects the effectiveness of reconnaissance, but also affects the flight costs. In order to ensure the effectiveness of reconnaissance, it is necessary to allocate reconnaissance time reasonably.

Under the constraint of UAV flight time, the sequence of tasks executed only affects the time of the second half of the flight. When the planning of the task sequence is completed, the reconnaissance time $\sum_{k=1}^{|P_j|} t_{p_{j,k}}$ that UAV $_j$ can be allocated

Algorithm 3 Time Allocation for Reconnaissance Targets Based on GP

Input: Reconnaissance target time upper bound Tm_j and UAV task sequence P_j

Output: Reconnaissance target time allocation vector \mathbf{t}

- 1: **Initialization:** Let $iter = 0$, define the maximum number of iterations $iter_{max}$, accuracy ϵ , and initialize $\mathbf{t}^{(0)}$
- 2: **repeat**
- 3: Calculate the gradient: $\nabla_t \xi(\mathbf{t})$
- 4: Calculate the projection: $\mathbf{t}_{proj} = P_{\Omega_B}(\mathbf{t} - \nabla_t \xi(\mathbf{t}))$
- 5: Update the vector: $\mathbf{t} \leftarrow \mathbf{t} + \gamma(\mathbf{t}_{proj} - \mathbf{t})$, where γ is the step size
- 6: **until** The maximum number of iterations is reached

has an upper bound Tm_j , which is denoted by

$$Tm_j = Tf_j - \frac{1}{v_0} \left[d(p_{j,k}, p_{j,0}) + \sum_{k=0}^{n-1} d(p_{j,k}, p_{j,k+1}) \right] \quad (24)$$

The objective function is thus formulated as follows:

$$\xi(\mathbf{t}) = \sum_{k=1}^{|P_j|} \alpha \left(I_{kp_{j,k}} + A_{p_{j,k}} \cdot I_{up_{j,k}} \frac{e^{t_{p_{j,k}}} - 1}{e^{t_{p_{j,k}}} + 1} \right) - \beta t_{p_{j,k}} \quad (25)$$

The problem can be expressed as an optimization problem for a nonlinear function:

$$\begin{aligned} & \min -\xi(\mathbf{t}) \\ & \text{s.t. } \sum_{k=1}^{|P_j|} t_{p_{j,k}} \leq Tm_j \\ & \quad t_{p_{j,k}} \geq 0 \end{aligned} \quad (26)$$

The first constraint ensures that the total allocated time does not exceed Tm_j , while the second constraint guarantees that the allocated time for each reconnaissance target is non-negative. The problem can be equivalently transformed into solving the minimum of the inverse of the original objective function by seeking to find the maximum value of the original objective function:

$$\Phi(x) = -\xi(x) = \beta x - \alpha \left(I_{kp_{j,k}} + A_{p_{j,k}} I_{up_{j,k}} \frac{e^x - 1}{e^x + 1} \right) \quad (27)$$

Theorem 2: The function $\Phi(x)$ is convex.

Proof: To simplify the proof, consider $\Phi(x) = \beta x - (a + b \frac{e^x - 1}{e^x + 1})$ of x , where $a = \alpha I_{kp_{j,k}}$ and $b = \alpha A_{p_{j,k}} I_{up_{j,k}}$. The second derivative of $\Phi(x)$ is computed as follows:

$$\Phi'(x) = \beta - \frac{2be^x}{(e^x + 1)^2}, \quad \Phi''(x) = \frac{2b(e^{2x} - e^x)}{(e^x + 1)^3} \quad (28)$$

Since $\Phi''(x) > 0$ for $x > 0$, concluding that the function $\Phi(x)$ is convex. ■

As the objective function of the problem is a sum of $\Phi(t)$, it is also convex with respect to t , and the constraints are independent probability simplex. If the sequence of UAV task execution is determined, the GP based method is employed for allocating time to reconnaissance targets. The GP method is shown in **Algorithm 3**.

Let $t \in \Omega_t$ where

$$\Omega_t \triangleq \left\{ \sum_{k=1}^{|P_j|} t_{p_{j,k}} \leq Tm_j, t_{p_{j,k}} \geq 0, \forall j \right\} \quad (29)$$

given a vector $\bar{\mathbf{t}} \in \mathbb{R}^{|P_j|}$, the projection of $\bar{\mathbf{t}}$ onto the simplex Ω_t is equal to

$$\mathbf{t} = \arg \min_{\mathbf{t} \in \Omega_t} \|\mathbf{t} - \bar{\mathbf{t}}\| \quad (30)$$

denote the projection as $P_{\Omega_B}(\bar{\mathbf{t}})$.

The optimal allocation of reconnaissance target time for the aforementioned problem can be obtained by iteratively computing the gradient projection update vector \mathbf{t} .

E. Complexity Analysis

In **Algorithm 1**: The outer loop iterates over the length of N UAVs, while the inner loop iterates over the length of M Target. The operations within the inner loop mainly involve basic condition judgments and information storage, resulting in a time complexity of $\mathcal{O}(M \times N)$ for both loops combined. Therefore, the time complexity of **Algorithm 1** is $\mathcal{O}(M \times N)$.

In **Algorithm 2**: The initialization phase primarily consists of assignments and a fixed number of iterations, resulting in a constant time complexity $\mathcal{O}(1)$. The outer loop iterates for k_{max} times, while the inner loop iterates for $N_{particles}$ times. Within the inner loop, mathematical operations and conditional judgments are performed, leading to a time complexity of $\mathcal{O}(N_{particles})$ and $\mathcal{O}(k_{max} \times N_{particles})$ respectively for the inner and outer loops. Consequently, the total time complexity of **Algorithm 2** is $\mathcal{O}(k_{max} \times N_{particles})$.

In **Algorithm 3**: The number of iterations is limited by $iter_{max}$. During each iteration, vector and matrix operations are involved with a time complexity of $\mathcal{O}(N)$. Hence, the time complexity of **Algorithm 3** is $\mathcal{O}(iter_{max} \times N)$.

In **Algorithm 4**: The initialization phase has a constant time complexity $\mathcal{O}(1)$. For the loops in this algorithm, in worst-case scenarios where N UAVs need to be traversed, each iteration has a constant time complexity $\mathcal{O}(1)$. Looping over all N UAVs results in an overall linear time complexity $\mathcal{O}(N)$. Additionally, updating the sequence of tasks also has a constant time complexity $\mathcal{O}(1)$. Hence, the time complexity of **Algorithm 4** is $\mathcal{O}(N)$.

There is no increase in the time complexity of the algorithm as compared to the standard PSO algorithm.

IV. EXPERIMENT AND ANALYSIS

In this section, the validity of the established UAV reconnaissance task model and the proposed HTA is verified through simulation experiments. The simulation experiments are run in Python3.10 environment. Computer processor and memory parameters are AMD Ryzen 7 5800H with Radeon Graphics(16 CPUs), 3.2GHz and 16GB RAM. The simulation parameter Settings are shown in Table I.

TABLE II
SIMULATION PARAMETER SETTING

Parameter	Value
Reconnaissance target length and width	$L_T \in [5, 30]$ and $W_T \in [5, 30]$
The position coordinates of the reconnaissance target	$x \in [0, 200]$ and $y \in [0, 200]$
Information known before the investigation begins	$I_{ki} \in [0, 0.5]$
UAV reconnaissance radius	$r_i \in [6, 10]$
Maximum flight time of the UAV	$Tf_j \in [50, 200]$
UAV transition flight speed	$v_0 = 6$
UAV type versus target desired type	$Type_\lambda \in \{1, 2, 3\}$
Utility and cost weight coefficients	$\alpha = 5$ and $\beta = 0.01$

TABLE III
SIMULATION SCENARIO DESIGN

Number of scenarios	Number of UAVs	Number of targets		
		HT	SLT	SST
1	5	10	0	0
2	5	6	4	0
3	5	4	4	2
4	5	3	3	4

A. Comparative Analysis of Utility Experiments

The UAV reconnaissance task allocation scheme is evaluated in four scenarios during the simulation experiment, and the reconnaissance utility is compared with GACO [36] and MVO [34]. The specific details of each scenario are presented in Table II. The number of UAVs ($N = 5$) and the number of heterogeneous targets ($M = 10$) remain consistent across all 4 scenarios, while varying the number of heterogeneous targets for each type among different scenarios.

In Scenario 1, only HTs are considered, which is consistent with the scenarios used in common algorithms. In Scenario 2, SLTs are introduced to enhance the complexity. Scenario 3 and 4 incorporate different numbers of SSTs to simulate real reconnaissance environment, with the difference that scenario 4 contains more SSTs than scenario 3.

During the simulation, HTRA iterations will terminate if the number of algorithm iterations exceeds the maximum limit. For each scenario, 20 tests are conducted to calculate the average utility and evaluate the algorithm's performance in diverse scenarios.

1) *Schemes of Reconnaissance Task Allocation Under 4 Scenarios:* The schematic diagram of the UAV allocation scheme under Scenario 1 is depicted in Fig. 7(a). Additionally, the specific task schedules of each UAV can be observed in Fig. 7(b), Fig. 8(a), Fig. 9(a) and 10(a) which illustrate the schematics of the UAV allocation schemes under scenarios 2, 3, and 4 respectively. The corresponding specific task schedules are presented in Figs. 8(b), 9(b), and 10(b). Taking Fig. 7 as an example, Fig. 7(a) visually represents the temporal evolution of UAV positions, reflecting the sequential order of task execution for each UAV. In these figures, all tasks have been completed by the UAVs without any conflicts during execution, demonstrating successful task allocation and coordination achieved by our proposed UAV system.

Fig. 7(b) displays the specific task allocation schedule for each UAV, where the length of the rectangle indicates the

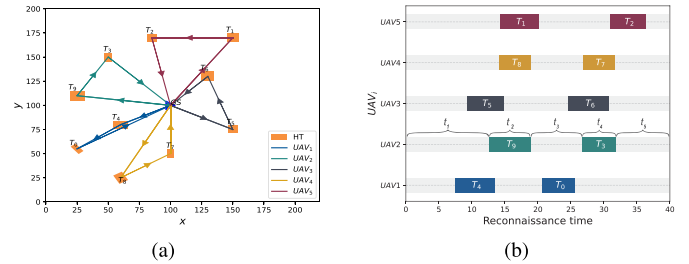


Fig. 7. Task allocation scheme under Scenario 1.

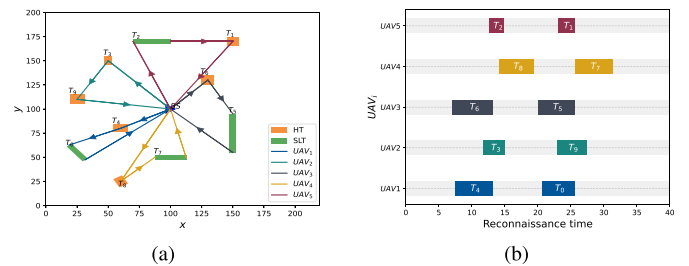


Fig. 8. Task allocation scheme under Scenario 2.

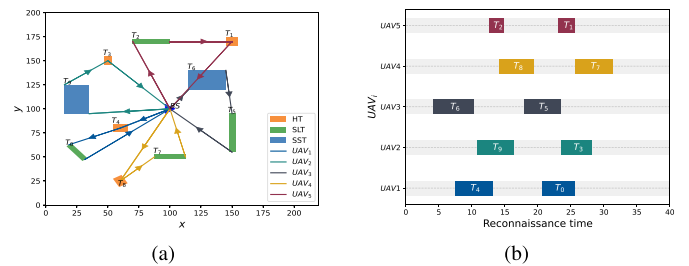


Fig. 9. Task allocation scheme under Scenario 3.

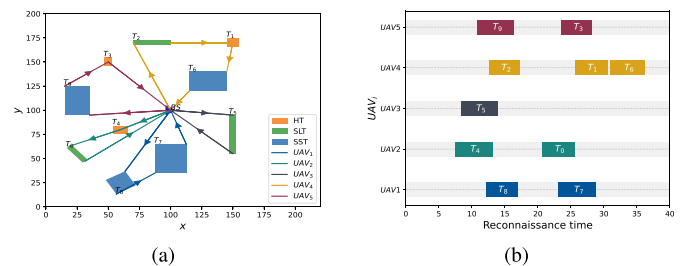


Fig. 10. Task allocation scheme under Scenario 4.

time window for executing the respective task. Take the task schedule of UAV₂ as an example: t_1 represents the time when UAV₂ flies from the BS to the target T_9 , t_2 represents the time

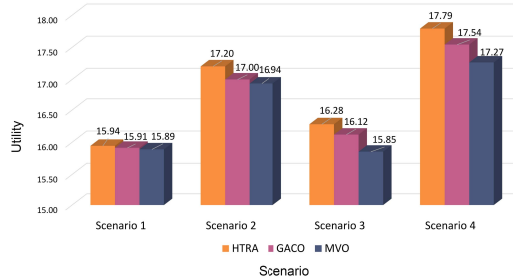


Fig. 11. Graph of comparison of algorithm utility in different scenarios.

to execute task T_9 , t_3 is the flight time from target T_9 to target T_3 , t_4 represents the time to execute task T_3 , t_5 represents the time to fly back to the BS from the target T_3 .

The figure illustrates that certain UAVs may perform multiple tasks during task allocation due to varying target requirements and UAV reconnaissance capabilities. By examining the task allocation scheme and the specific allocation time diagram for each UAV, it can be observed that the experimental results yield reasonable task allocations, effectively achieving the desired outcomes.

2) Reconnaissance Tasks Utility Under 4 Scenarios: The HTRA outperforms GACO and MVO in Scenarios 1 and 2 due to their relatively low complexity, which solely involves HTs and SLTs. When comparing the three algorithms' performance, the differences are not significant. However, the complexity of the environment increases significantly in Scenario 3 and 4, where SSTs are introduced. The proposed algorithm demonstrates more pronounced advantages over the other two algorithms.

B. Comparative Analysis of Reconnaissance Time and Utility

The optimal solution results of GP-based reconnaissance time allocation are compared with two commonly employed methods namely equal allocation and proportional allocation, in this section. This comparison aims to demonstrate the effectiveness of the HTRA method in achieving better task allocation outcomes.

- *Equal allocation:* Evenly allocation the time of each reconnaissance task. If there are N_T tasks and a remaining time T_M , then the remaining time is divided equally among each task, i.e., $t_i = T_M/N_T$.
- *Proportional allocation:* Proportional allocation is based on the unknown information of the reconnaissance target, with each task's time allocated proportionally according to its share of the total unknown information. This method ensures that tasks with more unknown information receive more dedicated time.

These two methods are compared with the solved optimal reconnaissance time allocation method. Fig. 12. shows a comparison of the total utility of the 3 methods under the four scenarios setting in Section IV.

Fig. 12. clearly shows that the total utility achieved by GP in all four scenarios is higher compared to the other two methods. The experimental results demonstrate that this

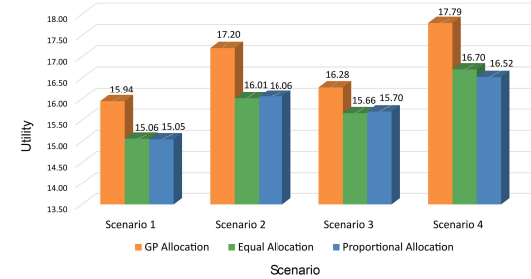


Fig. 12. Comparison graph of the relationship between the 3 time allocation methods and the utility.

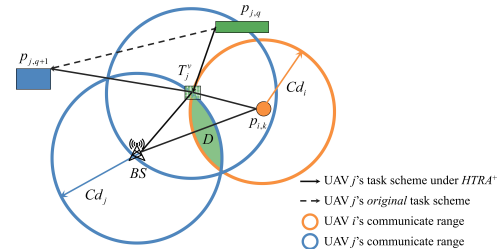


Fig. 13. Schematic diagram of the relay target location construction.

method effectively enhances the overall system utility compared to the equal allocation and proportional allocation. The ability of GP to optimize time allocation based on the specific requirements of each reconnaissance target contributes to its superior performance in maximizing the reconnaissance utility.

V. HTRA⁺ ALGORITHM

When the UAV is engaged in a task, if the distance between the current target and the BS exceeds a certain threshold, there be a potential risk of communication loss among different UAVs, thereby impeding real-time monitoring of some UAVs by the BS and leading to incomplete reconnaissance information. To address this problem, this section proposes an UAVs communication preservation model. This model involves creating a Virtual Target (VT) based on task requirements and implementing an auction mechanism to select a communication relay UAV. This ensures the integrity of reconnaissance task execution and enhances communication reliability among UAVs during task execution.

A. Communication Preservation Model

In order to realize communication preservation between BS and UAV_i , the concept of communication relay is introduced in the model. Let t_i^r represents the remaining time for UAV_i to return to the BS after executing task $p_{i,k}$, and let Cd_i denotes the maximum communication distance. When UAV_i performs the task $p_{i,k}$, it is necessary to introduce communication hold if the task location meets Equation (31).

$$Cd_i < d(0, p_{i,k}) \leq Cd_i + \max_{\forall j} Cd_j \quad (31)$$

As shown in Fig. 13, when UAV_i performs task $p_{i,k}$, the maximum communication distance Cd_i exceeds the distance between UAV_i and BS , and it cannot communicate with BS .

In this case, a virtual task T_j^v is created between $p_{i,k}$ and BS , and T_j^v is added to the task list to be executed. The relay task then uses an auction mechanism to select the drones that will perform the relay task. After the $p_{j,q}$ task, UAV_j first goes to T_j^v for relay task, and then to $p_{j,q+1}$ for reconnaissance task.

The construction of VT is divided into the following two types:

Case 1: If $Cd_i < Cd_j$, firstly, make a circle $\odot BS$ with base station as the center and the length of Cd_j as the radius; then, make a circle $\odot p_{i,k}$ with target $p_{i,k}$ as the center and the length of Cd_i as the radius; if $d(0, p_{i,k}) > Cd_i + Cd_j$, then there is no communication location that satisfies UAV_j; otherwise, when there is a UAV belonging to the region as follow:

$$D = \{(x, y) \mid (x, y) \in \odot BS \cap \odot p_{i,k}\} \quad (32)$$

When $d(0, T_j^v) \leq Cd_j$ and $d(T_j^v, p_{i,k}) \leq Cd_i < Cd_j$ are satisfied, therefore the relay target in region D satisfies the condition of 2-hop communication with the BS and the task $p_{i,k}$ to realize long-distance communication preservation.

Case 2: If $Cd_i > Cd_j$, the first step of the relay target construction method remains the same as in Case 1. But unlike Case 1, in the second step, a circle with the center at $p_{i,k}$ and the radius of Cd_j is created as $\odot p_{i,k}$. This adjustment is necessary because when $Cd_i > Cd_j$, a portion of region D constructed following the steps of Case 1 fails to facilitate two-way communication between UAV_i and UAV_j. In other words, UAV_i does not fall within the communication range of UAV_j. If $d(0, p_{i,k}) > 2Cd_j$, no feasible communication location satisfying UAV_j exists. Otherwise, if there is a UAV belonging to the subsequent region D' , where

$$D' = \{(x, y) \mid (x, y) \in \odot BS \cap \odot p_{i,k}\} \quad (33)$$

When $d(0, T_j^v) \leq Cd_j$ and $d(T_j^v, p_{i,k}) \leq Cd_j < Cd_i$ are satisfied, the relay target in the region D' satisfies the condition of two-way communication with the base station and the target $p_{i,k}$ to realize the long-distance communication preservation.

The state function of UAV_i at time t is denoted as $\Theta(i, t)$. When UAV_i is executing a task at time t , $\Theta(i, t) = 1$. Otherwise, it is idle, that is, $\Theta(i, t) = 0$. **Algorithm 4** is relay target auction algorithm based on communication persistence (RTAC). Here, $t_{j,q}^{\text{begin}}$ represents the time when UAV_j starts executing task q , and T_j^v represents the VT of UAV_j.

In the RTAC, the relay target is considered as a relay task, and the UAV performing the intermediate task is selected through an auction mechanism. The winning bidder executes the communication relay task in accordance with predefined rules, resulting in the revenue of VT . This iterative algorithm continues selecting relay targets until a suitable one is found or when additional drones need to be deployed from the BS .

B. Experiments Under Communication Preservation

In Fig. 14, the target completion rate is defined as the ratio of successfully completed tasks to the total number of tasks M . The experiments are based on the Scenarios 4 in Table III. When the time is 30.93 minutes, HTA is able to execute 9 targets and the other three models are able to execute 8 targets. At 44.78 minutes and 55.62 minutes, HTA⁺ executes the

Algorithm 4 RTAC Algorithm

Input: The sequence P_{before} of reconnaissance targets with communication preservation is ignored
Output: Reconnaissance target sequence P_{after} based on communication preservation

- 1: **Initialization:** The set of relay targets $RT \leftarrow \emptyset$
- 2: **if** $\Theta(j, t) = 1$ and UAV_j in D **then**
- 3: The UAV_j closest to D is selected as the relay target
- 4: **else**
- 5: **for** each UAV_j **if** $\Theta(j, t) = 0$ **do**
- 6: Let the last completed task of UAV_j be $p_{j,q}$
- 7: Select the point closest to the exit of task $p_{j,q}$ in region D to construct the virtual target T_j^v
- 8: Let the flight time difference be
- 9:
$$\Delta t = \frac{d(p_{j,q}, T_j^v) + d(T_j^v, p_{j,q+1})}{v_0} + t_{i,k} - (t_{j,q+1}^{\text{begin}} - t_{j,q}^{\text{begin}})$$
- 10: **if** $\Delta t \leq t_i^r$ and $t_{j,q}^{\text{begin}} + t_{j,q} + \frac{d(p_{j,q}, T_j^v)}{v_0} \leq t_{i,k}^{\text{begin}}$ **then**
- 11: $RT \leftarrow RT \cup \{j\}$
- 12: **end if**
- 13: **end for**
- 14: The UAV j closest to D is selected as the relay target
- 15: **end if**
- 16: **if** $RT = \emptyset$ **then**
- 17: A new UAV is added from the BS as a relay target
- 18: **end if**
- 19: Update tasks sequence: $P_{\text{before}} \leftarrow P_{\text{after}}$

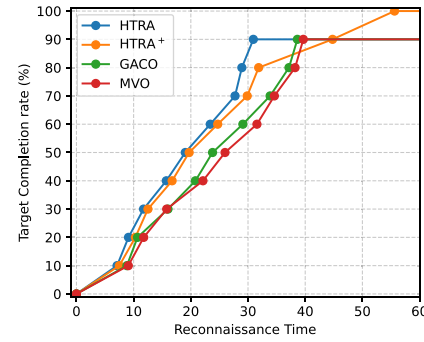
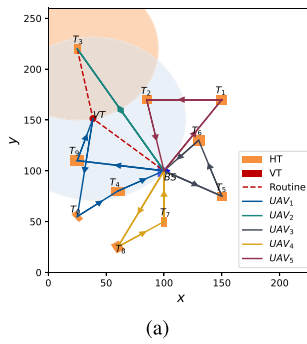


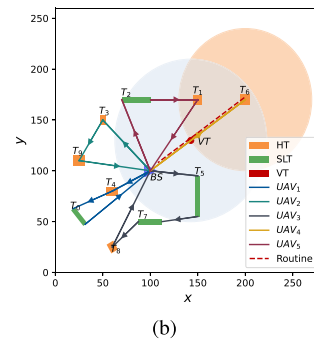
Fig. 14. The target completion rate comparison diagram.

9-th and 10-th tasks respectively. In contrast, the other three models lack a communication preservation, rendering them incapable of executing tasks over long distances.

In Fig. 14, it is the HTA model that first achieves 90% target completion rate, because the adoption of GP algorithm has relatively low computational complexity and effectively shorts the time of task allocation. With the increase of reconnaissance time, the target completion rate of HTA⁺ increases continuously and finally completes the reconnaissance task of all targets, which is higher than that of HTA, GACO and MVO. In real target-driven reconnaissance scenarios, objective factors such as long-distance communication cannot be ignored. By considering the relationship between target completion rate and time, HTA⁺ algorithm with communication preservation



(a)



(b)

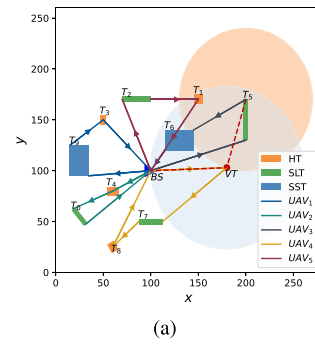
Fig. 15. Schematic diagram of the relay target location construction under Scenario 1& 2.

mechanism can detect more targets in the available time and ensure that all tasks can be executed.

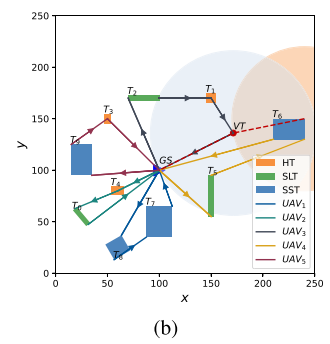
As shown in Fig. 15(a), UAVs execute the reconnaissance targets under communication preservation under Scenario 1, in which the position of target T_3 is changed to (25, 220). It is assumed that the maximum communication distance of UAV₁ is $Cd_1 = 80$ and the maximum communication distance of UAV₂ is $Cd_2 = 70$. Since the distance between target T_3 and the BS exceeds the maximum communication distance of UAV₂, UAV₂ will lose communication with the base station when detecting target T_3 , and the obtained reconnaissance information cannot be transmitted. Therefore, in order to realize the long-distance communication between UAV₂ and the base station, the VT is calculated and the coordinates is (38.56, 151.34). The blue line (flight path of UAV₁) indicates the experimental result of the task planning of the communication preservation mechanism after adding the relay role, the red point indicates the VT of UAV₁, and the red dashed line (Routine) represents the two-hop communication path of UAV₂.

It can be seen in Fig. 7(a), all UAVs can communicate with the BS normally. In Fig. 15, T_3 is assumed to be a further target, that is, UAV₂ cannot directly communicate with the BS when executing target T_3 . After introducing RTAC and establishing a VT, this communication relay task is auctioned. In this case, UAV₁ wins the bid, and UAV₁ goes to the VT after executing the reconnaissance target T_9 . The RTAC ensures that the investigation task can be transmitted effectively and the integrity of the investigation information can be obtained. Fig. 15(b) shows the communication preservation schematic under the Scenario 2. It can be clearly seen that UAV₄ cannot communicate directly with the base station when executing target T_6 . After introducing RTAC, there is currently no idle UAV that can execute the communication relay task, and then an additional UAV is dispatched from the base station to the VT. Finally, UAV₄ can communicate with the base station while executing the target T_6 .

Fig. 16(a) shows the communication preservation schematic under the Scenario 3. It can be clearly seen that when the target T_5 exceeds the communication distance of UAV₃ that is currently executing the task, UAV₄ becomes the relay target VT for communication preservation through the RTAC, enabling UAV₃ to successfully execute the target T_5 . Fig. 16(b)



(a)



(b)

Fig. 16. Schematic diagram of the relay target location construction under Scenario 3& 4.

shows the communication preservation schematic under the Scenario 4, it can be clearly seen that when the target T_6 exceeds the communication distance of the UAV₄ that is currently executing the task, through the RTAC, the UAV₃ becomes the communication preservation relay target VT, which enables the UAV₃ to successfully reconnoiter the target T_6 .

VI. CONCLUSION AND FUTURE WORK

The proposed HTA enables the allocation of UAVs reconnaissance tasks. By considering the heterogeneity of geometric features and target values, the heterogeneity of UAV performance, and the correlation between reconnaissance utility and time, HTA improves the total utility of UAVs reconnaissance tasks. Simulation results demonstrate that HTA outperforms GACO and MVO in terms of reconnaissance utility. In limited communication environment, HTA⁺ effectively handles long-distance reconnaissance targets and improve the task completion rate.

With their high stability, low cost and high implementability, UAVs will become the primary force for future reconnaissance tasks. Research can be further conducted in the following aspects:

- 1) Although this paper considers the reconnaissance of heterogeneous targets, it deals only with reconnaissance between static targets and not with dynamic targets, which can be taken into account in future research;
- 2) The implementation of methods on real UAVs poses challenges in terms of software integration with drone hardware, while adherence to regulatory and licensing requirements becomes imperative for algorithm deployment.
- 3) UAVs may encounter damages or emergencies when executing tasks in real scenarios. In the future, how UAVs cope with emergencies is a question to be explored.

REFERENCES

- [1] P. G. Fahlstrom, T. J. Gleason, and M. H. Sadraey, *Introduction to UAV Systems*. Hoboken, NJ, USA: Wiley, 2022.
- [2] S. Chen, F. Hu, Z. Chen, and H. Wu, "Correction method for UAV pose estimation with dynamic compensation and noise reduction using multi-sensor fusion," *IEEE Trans. Consum. Electron.*, early access, Dec. 11, 2023, doi: 10.1109/TCE.2023.3339729.

- [3] K. Obermeyer, "Path planning for a UAV performing reconnaissance of static ground targets in terrain," in *Proc. AIAA Guid., Navig., Control Conf.*, 2009, p. 5888.
- [4] M. Hu et al., "On the joint design of routing and scheduling for vehicle-assisted multi-UAV inspection," *Future Gener. Comput. Syst.*, vol. 94, pp. 214–223, May 2019.
- [5] M. Silvagni, A. Tonoli, E. Zenerino, and M. Chiaberge, "Multipurpose UAV for search and rescue operations in mountain avalanche events," *Geomat., Nat. Hazards Risk*, vol. 8, no. 1, pp. 18–33, 2017.
- [6] E. T. Alotaibi, S. S. Alqefari, and A. Koubaa, "LSAR: Multi-UAV collaboration for search and rescue missions," *IEEE Access*, vol. 7, pp. 55817–55832, 2019.
- [7] C. Liu and T. Szirányi, "Real-time human detection and gesture recognition for on-board UAV rescue," *Sensors*, vol. 21, no. 6, p. 2180, 2021.
- [8] M. Itkin, M. Kim, and Y. Park, "Development of cloud-based UAV monitoring and management system," *Sensors*, vol. 16, no. 11, p. 1913, 2016.
- [9] R. Shakeri et al., "Design challenges of multi-UAV systems in cyber-physical applications: A comprehensive survey and future directions," *IEEE Commun. Surveys Tuts.*, vol. 21, no. 4, pp. 3340–3385, 4th Quart., 2019.
- [10] X. Wu, Y. Yin, L. Xu, X. Wu, F. Meng, and R. Zhen, "Multi-UAV task allocation based on improved genetic algorithm," *IEEE Access*, vol. 9, pp. 100369–100379, 2021.
- [11] E. P. de Freitas, M. Bassó, A. A. S. da Silva, M. R. Vizzotto, and M. S. C. Corrêa, "A distributed task allocation protocol for cooperative multi-UAV search and rescue systems," in *Proc. Int. Conf. Unmanned Aircr. Syst. (ICUAS)*, 2021, pp. 909–917.
- [12] Z. Fu, Y. Mao, D. He, J. Yu, and G. Xie, "Secure multi-UAV collaborative task allocation," *IEEE Access*, vol. 7, pp. 35579–35587, 2019.
- [13] H. Luo, Z. Liang, M. Zhu, X. Hu, and G. Wang, "Integrated optimization of unmanned aerial vehicle task allocation and path planning under steady wind," *Plos one*, vol. 13, no. 3, 2018, Art. no. e0194690.
- [14] M. A. Nguyen, G. T.-H. Dang, M. H. Hà, and M.-T. Pham, "The min-cost parallel drone scheduling vehicle routing problem," *Eur. J. Oper. Res.*, vol. 299, no. 3, pp. 910–930, 2022.
- [15] Z. Zhou et al., "When mobile crowd sensing meets UAV: Energy-efficient task assignment and route planning," *IEEE Trans. Commun.*, vol. 66, no. 11, pp. 5526–5538, Nov. 2018.
- [16] B. D. Song, K. Park, and J. Kim, "Persistent UAV delivery logistics: MILP formulation and efficient heuristic," *Comput. Ind. Eng.*, vol. 120, pp. 418–428, Jun. 2018.
- [17] F. Ye, J. Chen, Y. Tian, and T. Jiang, "Cooperative task assignment of a heterogeneous multi-UAV system using an adaptive genetic algorithm," *Electronics*, vol. 9, no. 4, p. 687, 2020.
- [18] Y. Tang, Y. Miao, A. Barnawi, B. Alzahrani, R. Alotaibi, and K. Hwang, "A joint global and local path planning optimization for UAV task scheduling towards crowd air monitoring," *Comput. Netw.*, vol. 193, Jul. 2021, Art. no. 107913.
- [19] Q. Peng, H. Wu, and R. Xue, "Review of dynamic task allocation methods for UAV swarms oriented to ground targets," *Complex Syst. Model. Simul.*, vol. 1, no. 3, pp. 163–175, Sep. 2021.
- [20] B. Li, X. Qi, B. Yu, and L. Liu, "Trajectory planning for UAV based on improved ACO algorithm," *IEEE Access*, vol. 8, pp. 2995–3006, 2020.
- [21] Y. Wang, P. Bai, X. Liang, W. Wang, J. Zhang, and Q. Fu, "Reconnaissance mission conducted by UAV swarms based on distributed PSO path planning algorithms," *IEEE Access*, vol. 7, pp. 105086–105099, 2019.
- [22] N. Qi, Z. Huang, F. Zhou, Q. Shi, Q. Wu, and M. Xiao, "A task-driven sequential overlapping coalition formation game for resource allocation in heterogeneous UAV networks," *IEEE Trans. Mobile Comput.*, vol. 22, no. 8, pp. 4439–4455, Aug. 2023.
- [23] R. G. Smith, "The contract net protocol: High-level communication and control in a distributed problem solver," *IEEE Trans. Comput.*, vol. C-29, no. 12, pp. 1104–1113, Dec. 1980.
- [24] D. P. Bertsekas, "A new algorithm for the assignment problem," *Math. Program.*, vol. 21, no. 1, pp. 152–171, 1981.
- [25] N. Qi, Z. Huang, W. Sun, S. Jin, and X. Su, "Coalitional formation-based group-buying for UAV-enabled data collection: An auction game approach," *IEEE Trans. Mobile Comput.*, vol. 22, no. 12, pp. 7420–7437, Dec. 2023.
- [26] N. Qi et al., "Unity makes strength: Coalition formation-based group-buying for timely UAV data collection," in *Proc. IEEE Glob. Commun. Conf. (GLOBECOM)*, 2022, pp. 3712–3717.
- [27] Z. Qin, C. Dong, A. Li, H. Dai, Q. Wu, and A. Xu, "Trajectory planning for reconnaissance mission based on fair-energy UAVs cooperation," *IEEE Access*, vol. 7, pp. 91120–91133, 2019.
- [28] P. Iscold, G. A. S. Pereira, and L. A. B. Torres, "Development of a hand-launched small UAV for ground reconnaissance," *IEEE Trans. Aerosp. Electron. Syst.*, vol. 46, no. 1, pp. 335–348, Jan. 2010.
- [29] X. Du, Q. Guo, H. Li, and Y. Zhang, "Multi-UAVs cooperative task assignment and path planning scheme," *J. Phys. Conf. Ser.*, vol. 1856, no. 1, 2021, Art. no. 012016, doi: [10.1088/1742-6596/1856/1/012016](https://doi.org/10.1088/1742-6596/1856/1/012016).
- [30] H. Jiang, G. Wang, Q. Liu, P. Gao, and X. Huang, "Hierarchical multi-UAVs task assignment based on dominance rough sets," *Appl. Soft Comput.*, vol. 143, Aug. 2023, Art. no. 110445.
- [31] X. Zhang, K. Wang, and W. Dai, "Multi-UAVs task assignment based on fully adaptive cross-entropy algorithm," in *Proc. 11th Int. Conf. Inf. Sci. Technol. (ICIST)*, 2021, pp. 286–291.
- [32] M. Li, C. Liu, K. Li, X. Liao, and K. Li, "Multi-task allocation with an optimized quantum particle swarm method," *Appl. Soft Comput.*, vol. 96, Nov. 2020, Art. no. 106603.
- [33] J. C. Amorim, V. Alves, and E. P. de Freitas, "Assessing a swarm-GAP based solution for the task allocation problem in dynamic scenarios," *Expert Syst. Appl.*, vol. 152, Aug. 2020, Art. no. 113437.
- [34] Z. Wei and X. Zhao, "Multi-UAVs cooperative reconnaissance task allocation under heterogeneous target values," *IEEE Access*, vol. 10, pp. 70955–70963, 2022.
- [35] W. Zhu, L. Li, L. Teng, and Y. Wen, "Multi-UAV reconnaissance task allocation for heterogeneous targets using an opposition-based genetic algorithm with double-chromosome encoding," *Chin. J. Aeronaut.*, vol. 31, no. 2, pp. 339–350, 2018.
- [36] S. Gao, J. Wu, and J. Ai, "Multi-UAV reconnaissance task allocation for heterogeneous targets using grouping ant colony optimization algorithm," *Soft Comput.*, vol. 25, pp. 7155–7167, Feb. 2021.